

# Viscoelastic Properties of Nafion at Elevated Temperature and Humidity

M. BARCLAY SATTERFIELD, JAY B. BENZIGER

Department of Chemical Engineering, Princeton University, Princeton, New Jersey

Received 25 June 2008; revised 19 September 2008; accepted 2 October 2008

DOI: 10.1002/polb.21608

Published online in Wiley InterScience (www.interscience.wiley.com).

**ABSTRACT:** Tensile stress–strain and stress relaxation properties of 1100 equivalent weight Nafion have been measured from 23 to 120 °C at 0–100% relative humidity. At room temperature, the elastic modulus of Nafion decreases with water activity. At 90 °C, the elastic modulus goes through a maximum at a water activity of  $\sim 0.3$ . At temperatures  $\geq 90$  °C, hydrated membranes are stiffer than dry membranes. Stress-relaxation was found to have two very different rates depending on strain, temperature, and water content. At high temperature, low water activity, and small strain, the stress relaxation displays a maximum relaxation time with stress approaching zero after  $10^3$ – $10^4$  s. Water absorption slows down stress-relaxation rates. At high water activity, the maximum stress relaxation time was  $>10^5$  s at all temperatures. No maximum relaxation time was seen at  $T \leq 50$  °C. Increasing the applied strain also resulted in no observed upper limit to the stress relaxation time. The results suggest that temperature, absorbed water, and imposed strain alter the microstructure of Nafion inducing ordering transitions; ordered microstructure increases the elastic modulus and results in a stress relaxation time of  $>10^5$  s. Loss of microphase order reduces the elastic modulus and results in a maximum stress relaxation time of  $10^3$ – $10^4$  s. ©2008 Wiley Periodicals, Inc. *J Polym Sci Part B: Polym Phys* 47: 11–24, 2009.

**Keywords:** elastic modulus; microphase separation; Nafion; stress; stress relaxation; structure-property relations; thermal properties; transitions; viscoelastic properties

## INTRODUCTION

The mechanical properties of ionomer membranes employed in fuel cells play an important role in fuel cell performance.<sup>1–22</sup> Prolonged build-up of stresses from changes in temperature and membrane water content during dynamic cell operation has been identified as a key cause of mechanical failure of the membrane, either due to the formation of pin holes or delamination of the membrane from the electrode material,<sup>1–9</sup> and work to improve Nafion or find alternatives has begun to expand its original focus on membrane

conductivity and perm-selectivity to include durability and mechanical properties.<sup>5,6,10–12</sup> The elastic modulus is also known to affect equilibrium swelling and water sorption,<sup>10,13–15</sup> and stress-relaxation appears to correlate with water sorption dynamics.<sup>15–17,23–25</sup>

However, several researchers have pointed out there is a dearth of comprehensive information about the viscoelastic properties of fuel cell membranes, particularly at conditions relevant to fuel cell operation: elevated temperature and humidity.<sup>4–6,10</sup> This scarcity is not surprising, as most mechanical testing equipment can easily be configured to operate over a range of temperatures, but has little allowance for humidity control.

A summary of all work on elastic moduli reported through 2006 appears in Table 1.

Correspondence to: J. B. Benziger (E-mail: benziger@princeton.edu)

*Journal of Polymer Science: Part B: Polymer Physics*, Vol. 47, 11–24 (2009)  
© 2008 Wiley Periodicals, Inc.

**Table 1.** Summary Elastic Modulus (Young's Modulus) of Nafion

Researcher, Year	Material	Apparatus	Method	Water Content	Temp.	Elastic Modulus (MPa)
DuPont Product Information <sup>28</sup>	Nafion PFSA Mem- branes, N-112, NE- 1135, N-115, N-117, NE-1110		ASTM D 882	50% RH Water soaked	23 °C 23 °C 100 °C	249 114 64
Werner, Jorissen et al. 1996 <sup>19</sup>	Nafion 117, 50 mm length	Zwick 1445 Univer- salprüf-machine	Strain rate: 0.20/min in machine direction	Dry "Completely humidified"	25 °C 25 °C	~ 100 ~ 50
Kawano, Wang et al. 2002 <sup>29</sup>	Nafion 117, Aldrich, acid form, 25 mm length × 6 mm	T.A. Instruments DMA 2980, con- trolled force mode, tension	Preload force: 0.005 N, soak time: 1 min, force ramp rate: 0.500 N/min, upper force: 18.00 N	Unspecified Water soaked, 24 h Boiling water soaked, 1 h As-received	200 °C 27 °C 27 °C 27 °C 60 °C 90 °C 120 °C 150 °C 180 °C	~ 1 95 128 200 147 44 5 3 2
Kundu, Simon et al. 2005 <sup>6</sup>	Solution Cast Nafion 117, 5 mm gauge length × 6 mm	Rheometrics DMTA V, tension	Preload force: 0.1 N, strain rate: 0.001/ min, max strain: 0.015–0.024.	Water soaked	27 °C 60 °C 90 °C 120 °C 150 °C 180 °C 80 °C	210 176 80 13 4 2 ~ 45
Fujimoto, Hickner et al. 2005 <sup>30</sup>	Solution Cast Nafion 112 Nafion 117, 30 mm gauge × 9 mm	Com-Ten Industries 95T series load frame equipped, load cell: 200 lbf	Strain rate: 0.17/min	Ambient Soaked in water until tested	RT RT	~ 35 200 52
Kyriakides 2005 <sup>31</sup> , Liu, Kyriakides et al. 2006 <sup>5</sup>	Nafion 117; pretreated/ boiling 0.5 M H <sub>2</sub> SO <sub>4</sub> 2 h and boiling DI water 2 h, dried 70 °C vac- uum, 40 mm gauge length × 12 mm	Instron 4468 screw- driven universal testing machine, load cell: 1 kN	Strain rate: 0.7/min Strain rate: 0.3/min Strain rate: 0.12/min Strain rate: 0.07/min Strain rate: 0.025/min	Equilibrated at 23 °C, 40% RH 72 h, water concentration: 5.3 °C 1.5%	23 °C	270 ± 4 253 ± 7 256 ± 18 263 ± 10 250 ± 5

Generally, membranes at higher temperatures and higher water content exhibit a lower Young's modulus. Numbers with the “~” sign indicate values read from published curves.

Recent studies have improved the environmental control for mechanical testing. Tang et al.<sup>3</sup> used a custom temperature and humidity chamber installed on an MTS Alliance RT/5 material testing system, and tested Nafion 112 in 16 different environments: 25, 45, 65, 85 °C and 30%, 50%, 70%, and 90% relative humidity. They reported that the Young's modulus, ultimate stress and strain, and “proportional limit” all decreased with both temperature and water activity.

Choi et al.<sup>10</sup> used an optoelectronic holography technique, described in ref. 26, on Nafion 112 with varying sample length and a pre-experiment environmental conditioning period of 1 h.<sup>26,27</sup> They proposed that the Young's modulus  $E$  decreased exponentially as a function of the volume fraction of water in the polymer,  $\varepsilon_w$ .  $E = E_0 \exp[-2.1753\varepsilon_w]$ .  $E_0$  is the elastic modulus of Nafion at 0% RH and decreased from 316 MPa at 20 °C to 122 MPa at 90 °C. The results of Tang et al.<sup>3</sup> and Choi et al.<sup>14</sup> both suggest that increasing water and temperature decreases membrane stiffness. However, both those studies had a minimum relative humidity of 10–30%.

Bauer et al.<sup>4</sup> measured the storage and loss modulus for Nafion with a modified a TA Instruments DMA 2980, adding a custom-built humidity cell that maintained relative humidities of 0, 15, 50, 85, and 100% between room temperature and 100 °C. They found that the storage modulus of Nafion increased with decreasing water content at low temperatures, and that the storage modulus at all humidities decreased with increasing temperature. However, the modulus of the membrane tested at 0% RH decreased much faster with temperature than those at any humidity, eventually becoming significantly lower than the hydrated membranes. They also reported an increase in the elastic modulus of the protonated form of Nafion between dry conditions and low relative humidity.

Budinski and Gittleman et al.<sup>9</sup> performed dynamic tests on Nafion, using a both dry and wet Nafion 112. Their findings agree with those of Bauer et al.<sup>4</sup> and Uan-Zo-Li.<sup>18</sup> The storage modulus of the hydrated samples decreased with increasing temperature, but not as fast as that for dry samples. Also, the thermal transition seen at roughly 110 °C for dry Nafion does not appear to be lowered by the addition of water and may in

fact be raised, a result also reported by Bauer et al.<sup>4</sup> No thermal transition has been reported for Nafion at high water activity. The nature of this thermal transition has been ascribed to different phenomena by different investigators. Several investigators described it as the glass transition temperature.<sup>32–36</sup> Eisenberg and coworkers<sup>20,22,37</sup> and Moore and coworkers<sup>38</sup> both identified it with a order-disorder (melting) transition of ionic clusters (multiplets).

Recently, Majsztrik et al. developed an apparatus to measure creep and strain relaxation (creep recovery) in an environmentally controlled system.<sup>39,40</sup> Their results showed that water plasticized Nafion at low temperature, but water stiffened Nafion at higher temperatures. At 90 °C the creep rate of Nafion 1110 decreased by more than a factor of 100 between 0% RH and 85% RH. These results agreed qualitatively with those of Bauer, but the changes in creep with water activity at 90 °C were much more dramatic than seen by Bauer et al. and Budinski et al. Majsztrik et al. pointed out that environmental control is critical but also very difficult. The Bauer et al., Budinski et al., and Majsztrik et al. studies suggest that there has not been sufficient control over the environmental conditions in mechanical testing of Nafion.

Environmental control is also critical to the relaxation processes in Nafion. Yeo and Eisenberg<sup>22</sup> performed stress-relaxation tests on Nafion 1365 and observed a distribution of relaxation times. They reported that addition of a small amount of water (0.5 H<sub>2</sub>O/SO<sub>3</sub><sup>-</sup>) increased the stress-relaxation rate. These authors also reported that time-temperature superposition “broke down” with the addition of water, particularly at long times. This behavior was attributed to water plasticizing the ionic domains in Nafion, possibly adding or triggering alternative relaxation mechanism when introduced into the completely dry Nafion.

Liu and Kyriakides<sup>5</sup> performed stress-relaxation tests under ambient conditions (23 °C and 40% RH) at different strains and strain rates. At strains at and below the yield point of 7.6%, the authors noted divergence from the linear behavior observed at higher strains. They postulated that this was due to “the softening effect of a small amount of water uptake at the beginning of the stress-relaxation process.”<sup>5</sup>

Liu and Hickner<sup>7</sup> measured stress relaxation at ambient conditions and underwater or at two different strains. The absolute stress of the

submerged sample was lower, and the stress-relaxation rates were slower for the submerged sample. The authors postulated that because water plasticized the membrane and reduced the stress, the driving force for stress relaxation was lower, causing the slower rate.<sup>7</sup> The result that stress relaxation is slowed in hydrated Nafion, combined with results from Bauer et al.<sup>4</sup> and Uan-Zo-Li<sup>18</sup> highlights an unpredicted influence of water on the viscoelastic properties of Nafion that will be further explored in this work.

## EXPERIMENTAL

Extruded Nafion<sup>®</sup> 115 films (DuPont product, equivalent weight 1100 g polymer/mol SO<sub>3</sub><sup>-</sup>, 127 μm thickness) were obtained from Ion Power (New Castle, Del). All membranes were cleaned and ion-exchanged by boiling for 1 h in 3% H<sub>2</sub>O<sub>2</sub> in water, 20 min in deionized water, 1 h in 1M sulfuric acid and 20 min in deionized water. As received membranes have a yellow-brown tinge, boiling in hydrogen peroxide renders them clear and colorless. We have found that extruded membranes that have been boiled in sulfuric acid and hydrogen peroxide as described above show no memory of orientation or previous annealing and drying.

Experiments in this laboratory<sup>13,41</sup> have measured the equivalent weight by soaking the membranes in NaCl solution and then titrating the solution to determine the number of protons released during exchange; the equivalent weight of nearly 1100 g polymer per mole acid is routinely reproduced.

After cleaning and ion-exchanging, the membranes were stored at room temperature and 100% relative humidity. Membranes were die-punched into dogbone samples, overall dimensions: 3.81 × 1.59 cm, gauge dimensions: 2.25 × 0.475 cm. Because Nafion's dimensions change with water content, care was taken to equilibrate the Nafion at the water content of interest before die-punching.

### Stress–Strain Measurements

Stress–strain experiments were performed in an Instron 1122 tensile tester, with an Instron model 3111 environmental chamber, pictured in Figure 1.

To test membranes at room temperature and varying water activity, membranes were conditioned over saturated salt solutions at humidities of 6% (LiBr), 6% (NaOH), 9% (KOH), 29% (CaCl<sub>2</sub>),



**Figure 1.** Instron 1122 and environmental chamber used for stress–strain tests. The plastic bag vapor barrier was installed to for elevated humidity tests. [Color figure can be viewed in the online issue, which is available at [www.interscience.wiley.com](http://www.interscience.wiley.com).]

33% (MgCl<sub>2</sub>), 38% (NaI), 51% (Ca(NO<sub>3</sub>)<sub>2</sub>), 60% (NaNO<sub>2</sub>), 63% (MnCl<sub>2</sub>), 75% (NaCl), 84% (KCl), 94% (CuSO<sub>4</sub>), and 97% (K<sub>2</sub>SO<sub>4</sub>)<sup>42,43</sup> for at least 2 wk. Four membranes were tested at each pre-equilibrated water activity. Three membranes were also tested after each of: 1 day of immersion in liquid water, 1 h of immersion in boiling water and 1 day and 2 wk of equilibration with water vapor at 100% humidity. Membranes were removed from the controlled humidity and tested under ambient conditions of ~ 23 °C and ~ 40% RH. Testing was completed in ~ 2 min, and membranes were weighed before and after the test to determine their water content during the test. The wettest membranes (boiled in water) lost at most 30% of their initial water during the tests (corresponding to a decrease from 20 to 15 in λ = number of waters per sulfonic acid residue), whereas the dry membranes gained at most 2.5% of their initial weight (corresponding to a gain of λ = 1.5). Average weight loss was λ < 2.5 for the wet samples and average weight gain was λ < 0.8 by the dry samples.

To better test membranes at elevated temperature and humidity, samples were placed in a 1-gallon sealed plastic bag with ~ 100 mL of water and clamped in the sample grips of the Instron machine through the bag, as pictured in Figure 1. The bag was kept slack so as not to interfere with

the test, and runs with an empty bag at different temperatures indicated that the effects of the bag on the reading were minimal, amounting to a maximum error of <1 MPa in the stress measurements.

Experiments reported here were run at a constant extension rate of 50 mm/min (2.28/min strain rate). A limited number of tests were performed at room temperature and ambient relative humidity at strain rates: 12.7, 2.5, and 0.5 mm/min. The effect of strain rates was minimal and was not pursued further. A selected number of tests were carried out with samples cut longitudinal and transverse to the machine direction of the extruded films. After the cleaning and pretreatment procedures, no effect of the sample orientation was observed. Details of these results can be found in chapter 2 Barclay Satterfield's thesis, which is available at <http://pemfc.princeton.edu/theses.html>.

### Stress Relaxation

Relaxation tests were performed in an Instron 5865 testing machine with an Instron 3111 environmental chamber. Samples were tested at ambient humidity ( $\sim 35\%$  RH at  $25^\circ\text{C}$ ) or in sealed bags at  $\sim 100\%$  RH or  $\sim 0\%$  RH (with Drierite<sup>®</sup> desiccant) at different temperatures. For the elevated humidity tests, Nafion was stored at room temperature and 100% RH after being cleaned, then removed and cut to the dogbone size. The sample and bag were then loaded into the Instron and allowed to equilibrate for at least 2 h at the test temperature. For dry tests, Nafion was dried at  $70^\circ\text{C}$  over Drierite for 2 h after being cleaned, stored at room temperature over Drierite, then removed and cut to dogbone size.

The samples all had the same initial gauge length at the test conditions of interest. However, the sample thickness varied by up to 10% between samples at 0% RH and those at 100% RH resulting from volumetric expansion of the Nafion due to water absorption. We did not correct the engineering stresses for this variation, and all the stress values reported are based on the nominal 127  $\mu\text{m}$  thickness.

After equilibration the gauge length was adjusted until the sample appeared taut. The gauge length was then readjusted, the load cell baseline "zeroed," then the test was started. The membranes were strained at 50%/s to preselected strains of 2, 5, 10, and 20% and held at constant strain while the stress was monitored; the initial

straining took 0.04–0.4 s. Stress was logged starting when the membrane was strained. Data points were recorded at 2 Hz for the first 1000 s and at 0.2 Hz for 1000–30,000 s. The initial stresses were recorded at 1 s after start of straining for the 2 and 5% tests to determine Young's modulus and added to the data gained through constant strain-rate tests. About half the test conditions were repeated, but in many cases, only one membrane was tested at each strain, temperature, and humidity condition.

### Data Analysis

The modulus ( $E$ ) was calculated from the slope of the stress( $\sigma$ )–strain( $\varepsilon$ ) curve ( $E = \partial\sigma/\partial\varepsilon$ ). The initial slope (small strain region) is the elastic or Young's modulus. The elastic modulus was also evaluated and from the initial stresses in the 2 and 5% strain–stress relaxation tests. Proportional stress and strain were point where the stress–strain curve first deviated from the linear region. Yield stress and strain were taken either from a local maximum in the transitions region between elastic and plastic deformation or, when a local maximum did not occur, as the point where the maximum rate of change of the modulus with strain occurred ( $\varepsilon_{\text{yield}}$  is the root to  $\partial^3\sigma/\partial\varepsilon^3 = 0$ , this was determined from the root of the third derivative of a 4th-order polynomial fit to the data in that region). The "plastic" modulus was defined as the slope of the linear portion of the stress–strain curve after yielding. Figure 2 illustrates the definitions of these quantities for stress–strain curves characteristic of Nafion at low and high water activity.

## RESULTS

### Stress–Strain Characterization

The stress–strain curves of Nafion obtained at room temperature and different water activities are illustrated in Figure 3. We have limited the number of relative humidities displayed in Figure 3 to reduce the complexity. The entire set of relative humidities studied can be found in Dr. Satterfield's thesis, which is available on the web at <http://pemfc.princeton.edu/theses.html>. The obvious trend is that the initial slope, which is the elastic modulus, decreases with increasing water activity. Nafion becomes less stiff with increasing water content. More careful examination of the Figure 3 reveals two features not previously

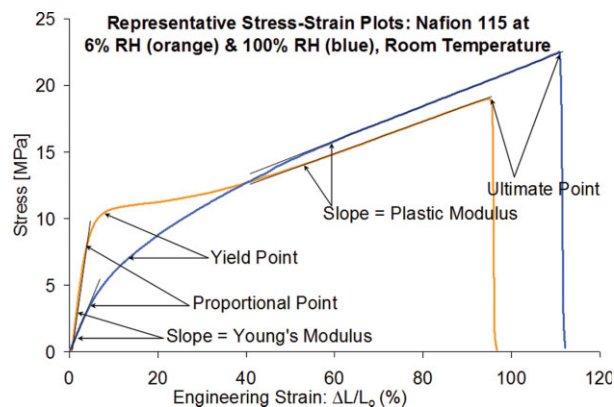


**Figure 2.** Definitions of the tensile properties for Nafion. The yield point is determined by finding where the third derivative of the stress–strain curve goes to zero.

reported. First, the stress–strain curve show plasticization continues to evolve over a 2-wk period with exposure to water vapor at room temperature. Figure 3 shows that placing the sample in liquid water at room temperature speeds up the plasticization process, and placing Nafion in boiling water further reduces the stiffness of the Nafion compared to having Nafion is 100% RH vapor for 2 wk. Second, the yield stress went through a maximum near  $a_w = 0.3$ . In addition to the maximum in yield stress, the elastic modulus was almost constant for water activity  $a_w < 0.3$ , and then decreases at higher water activity. The elastic modulus and yield stress appeared to

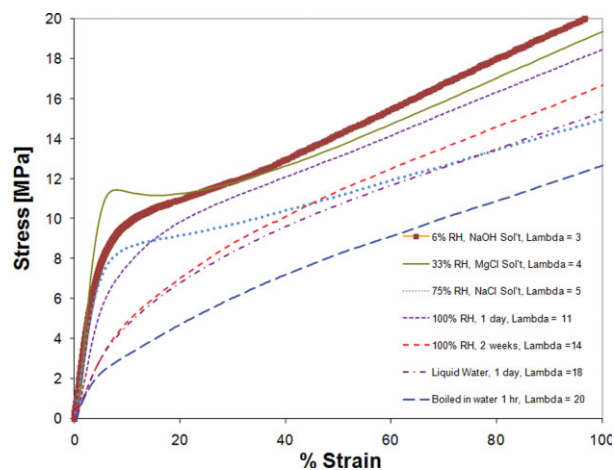


**Figure 3.** Stress–strain curves for 1100 equivalent weight Nafion at 23 °C as a function of water activity. Tests were done at a strain rate of  $2.28 \text{ min}^{-1}$ .

change in tandem with the water activity, both increased slightly as  $a_w$  increased from 0 to 0.3 and then decreased at higher water activity. This correlation of modulus and yield stress with water activity and the maximum at  $a_w = 0.3$  is shown more explicitly in Figure 4 where the yield stress and elastic modulus at 23 °C are plotted as functions of water activity. There is no change or a slight increase in elastic modulus between  $a_w = 0$  and  $a_w = 0.3$  and then the elastic modulus decreases at higher water activity.

Figure 5 summarizes the stress–strain tests for Nafion at 90 °C, both the elastic modulus and yield stress are plotted as functions of water activity. At low water activity ( $a_w < 0.35$ ) the elastic modulus is reduced by a factor of 3 and the yield stress is reduced by a factor of 2 compared to the values at 23 °C. There is a distinct maximum in the elastic modulus and yield stress as a function of water activity at  $a_w = 0.3$ . The elastic modulus and yield stress decrease much less with increased water activity at 90 °C than at 23 °C ( $(\partial E/\partial a_w)_{T=90, a_w > 0.3} < (\partial E/\partial a_w)_{T=23, a_w > 0.3}$ ). At 90 °C, the elastic modulus of Nafion at high water activity,  $a_w > 0.95$  is greater than the elastic modulus at 23 °C

$$\begin{aligned} E(T \geq 90^\circ, a_w = 0.95) &> E(T \geq 90^\circ, a_w = 0); \\ E(T < 90^\circ, a_w = 0.95) &< E(T < 90^\circ, a_w = 0). \end{aligned}$$

At low temperature water reduces the elastic modulus of Nafion (plasticizes), yet at high temperature water increases the elastic modulus (stiffens). This is shown more clearly in Figure 6

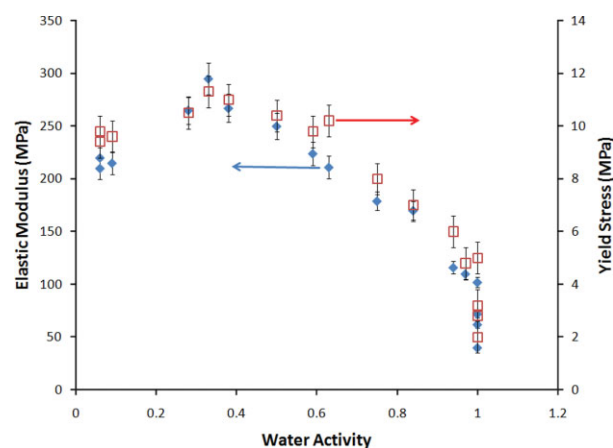


**Figure 4.** Elastic modulus and yield stress of 1100 equivalent weight Nafion at 23 °C as a function of water activity.

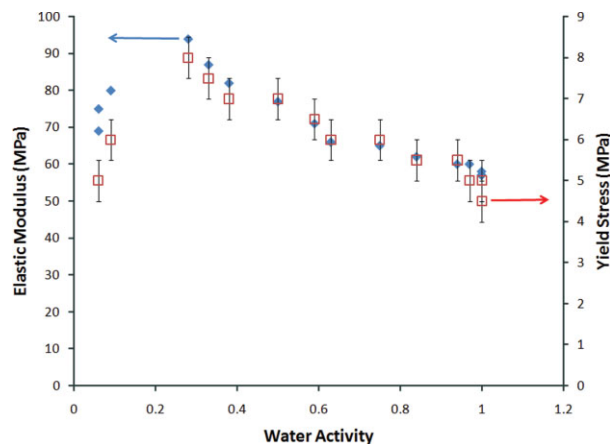


**Figure 5.** Elastic modulus and yield stress of 1100 equivalent weight Nafion as a function of water activity at 90 °C. [Color figure can be viewed in the online issue, which is available at [www.interscience.wiley.com](http://www.interscience.wiley.com).]

where the elastic moduli of Nafion at 100% RH and 0% RH are plotted as functions of temperature. Above 90 °C, the elastic modulus is greater at  $a_w = 1.0$ , and below 90 °C the elastic modulus is greater at  $a_w = 0$ . Unfortunately, with the flexible bags, we could not carry out tests above 95 °C with liquid water; experiments were carried out up to 120 °C at low water activity.

### Stress Relaxation of Nafion

The stress relaxation of Nafion was measured as a function of temperature at dry (0% RH) and humid (100% RH) conditions and at strains ( $\epsilon$ ) of 2, 5, 10, and 20%. Data were also collected for am-

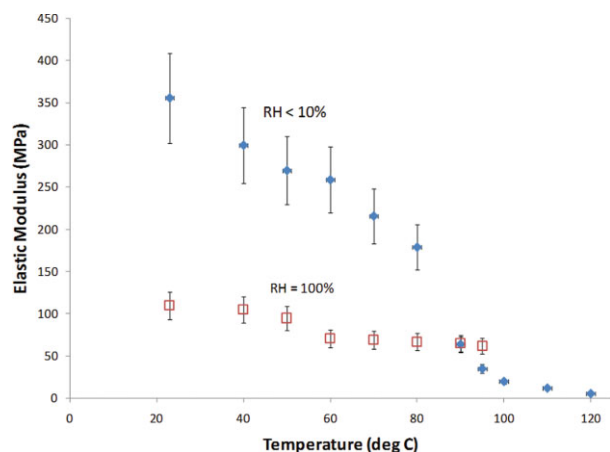


**Figure 6.** Elastic modulus of 1100 equivalent weight Nafion as a function of temperature at 100% RH and ~0% RH. [Color figure can be viewed in the online issue, which is available at [www.interscience.wiley.com](http://www.interscience.wiley.com).]

bient air (~35% RH at 23 °C) heated to higher temperatures. Heating ambient air produced nearly dry conditions at higher temperatures; above 60 °C ambient water activity is reduced to  $a_w < 0.03$ . Relaxation data are presented as log(modulus) versus log(time). The stress relaxation as a function of temperature at  $\epsilon = 5\%$  is summarized in Figure 7. The initial modulus at  $t = 0.5$  s decreases with increasing temperature ( $(\partial E/\partial T)_{a_w, t=0} < 0$ ). Stress relaxation curves, shown in Figure 11, display two distinctively different behaviors. All the stress relaxation curves for humid conditions show a nearly constant slope for all times up to  $10^5$  s, ( $d \log(E)/d \log(t) \approx \text{constant}$ ). In addition, the stress relaxation curves for dry conditions at 30 and 50 °C also have a constant slope. In contrast, the stress relaxation curves for dry conditions at 70 and 90 °C both show a large change in the slope at times of 100–1000 s. This distinction is highlighted in Figure 8 where the slope of the log(modulus) versus log(time) curves have been plotted as a function of time. These results show that, at low temperature and with high water activity, the log( $E$ ) line decays linearly with log(time); however, at 0% RH and high temperature, there appears to be a time where log( $E$ ) appears to decay rapidly towards zero. We will refer to the time where log( $E$ ) decays rapidly towards zero as the “stress relaxation time.”

The most surprising result is the crossing of the stress relaxation curves for wet and dry Nafion at 70 °C. At  $T \leq 50$  °C and 5% strain the modulus at  $a_w = 0$  is greater at all times than the

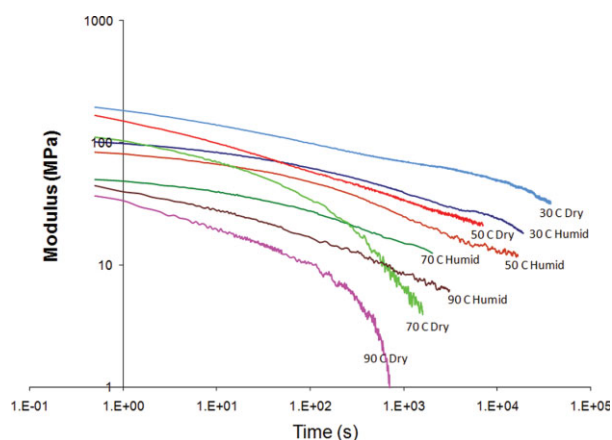


**Figure 7.** Stress relaxation for 1100 equivalent weight Nafion as a function of temperature and water activity. The initial strain was 5%. [Color figure can be viewed in the online issue, which is available at [www.interscience.wiley.com](http://www.interscience.wiley.com).]

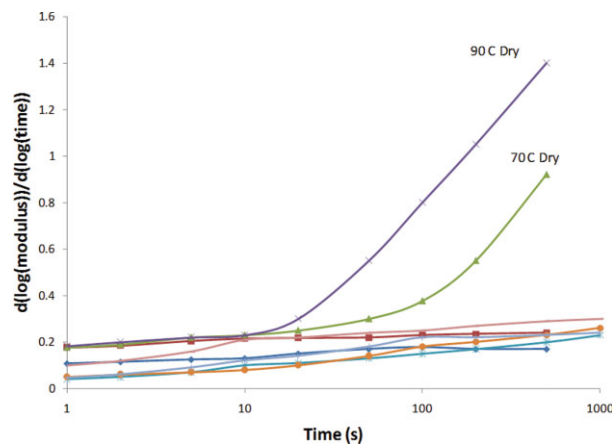


**Figure 8.** Plot of the slope of the relaxation curves shown in Figure 7 to highlight the difference in relaxation as a function of temperature and water activity. [Color figure can be viewed in the online issue, which is available at [www.interscience.wiley.com](http://www.interscience.wiley.com).]

modulus at  $a_w = 1.0$ . At 70 °C, the modulus at  $a_w = 0$  is initially greater than the modulus at  $a_w = 1.0$ , but the relaxation rate accelerates with time at  $a_w = 0$  and for  $t > 500$  s the modulus at  $a_w = 0$  is less than at  $a_w = 1.0$ . At 90 °C, the modulus for dry Nafion is always less than the modulus for wet Nafion, but it also shows the accelerated stress relaxation seen at 70 °C. At both 70 and 90 °C, there appears to be an upper limit to the stress relaxation time at  $a_w = 0$ ; the stress is dissipated after  $\sim 10^3$ – $10^4$  s, whereas the samples in a humid environment,  $a_w = 1.0$ , display no limit to the stress relaxation time up to  $10^5$  s.

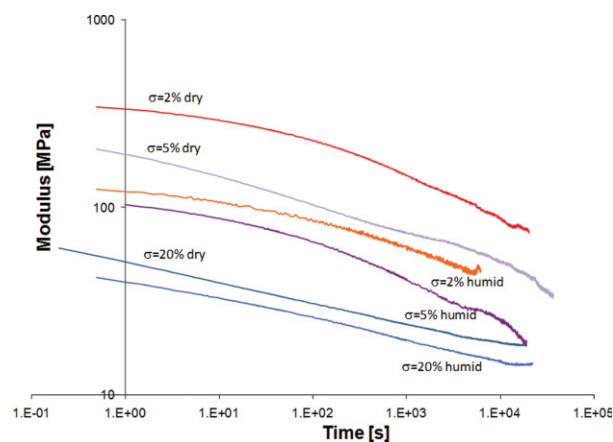


**Figure 9.** Stress relaxation of 1100 equivalent weight Nafion at 30 °C as a function of water activity and initial strain. Humid corresponds to 100% RH and dry corresponds to  $\sim 0\%$  RH. [Color figure can be viewed in the online issue, which is available at [www.interscience.wiley.com](http://www.interscience.wiley.com).]

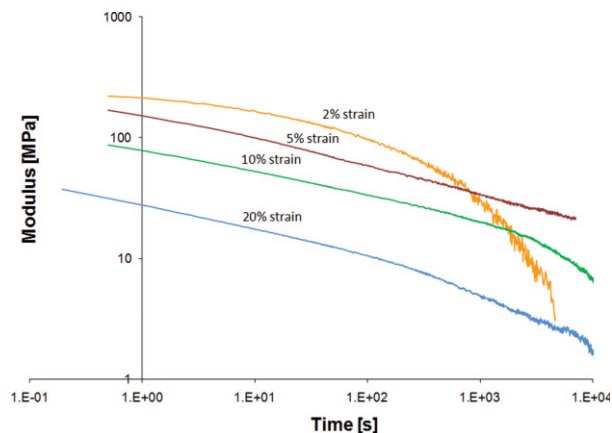


**Figure 10.** Stress relaxation of 1100 equivalent weight Nafion at 50 °C as a function of initial strain under dry conditions ( $\sim 0\%$  RH). [Color figure can be viewed in the online issue, which is available at [www.interscience.wiley.com](http://www.interscience.wiley.com).]

The relaxation rates show a complex dependence on both temperature and initial strain. Figures 9–11 show the stress relaxation of dry Nafion as a function of the initial strain at 30, 50, and 70 °C. At 30 °C (Fig. 9), the modulus always decreases with increasing strain at all times. At 50 °C (Fig. 10), the initial modulus decreases with increasing initial strain; however, the stress relaxation accelerates with time after a 2% strain, so that after 1000 s the stress at 2% initial strain becomes less than the stress at 5% initial strain, it becomes less than the stress after 10% initial strain after 2000 s, and it appears that the stress

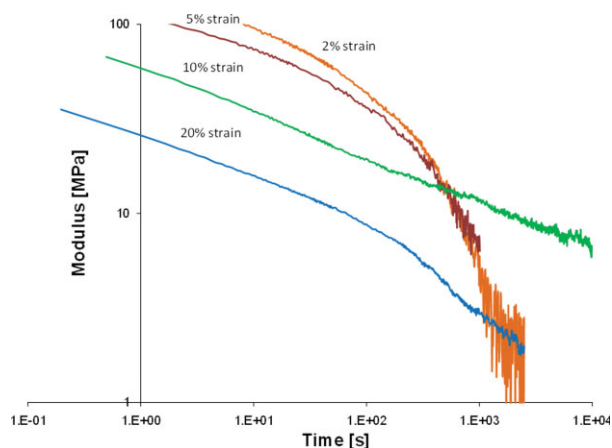


**Figure 11.** Stress relaxation of 1100 equivalent weight Nafion at 70 °C as a function of initial strain under dry conditions (0% RH). [Color figure can be viewed in the online issue, which is available at [www.interscience.wiley.com](http://www.interscience.wiley.com).]



at 2% initial strain would become less than the stress at 20% initial strain after 5000 s. At 70 °C (Fig. 11), the stress relaxation accelerated after both 2 and 5% initial strain so the stress relaxation curves crossed the stress relaxation curves after 10 and 20% initial strain.

Stress relaxation is also temperature and initial strain dependent for wet Nafion, but the stress relaxation curves do not cross. Figure 9 shows that at 30 °C the stress relaxation curves for wet Nafion have decreasing stress as a function of increasing initial strain at all times. In contrast, the stress relaxation at 90 °C (Fig. 12) shows the stress relaxation curves at the different initial strains relax to a single relaxation rate after  $\sim 1000$  s. The relaxation of wet Nafion after 1000 s does not show any evidence of acceleration, even at 90 °C, which is distinctly different than the relaxation of dry Nafion.

## DISCUSSION

Nafion displays some unusual tensile stress-strain behavior. The main points are summarized below:

1. Initial water absorption at  $0 < a_w < 0.3$  increases the yield stress of Nafion and elastic modulus of Nafion at both 23 and 90 °C. The elastic modulus of Nafion decreases for  $a_w > 0.3$  at both 23 and 90 °C.
2. The elastic modulus decreases with temperature. The temperature coefficient is greater at low water activity than at high water activity. Below 80 °C, the elastic modulus of Nafion is greater at  $a_w = 0$  than at  $a_w = 1.0$ ; above 90 °C, the elastic modulus is smaller at  $a_w = 0$  than at  $a_w = 1.0$ .
3. Dry Nafion ( $a_w = 0$ ) strained to  $\leq 5\%$  above 70 °C shows a maximum relaxation time of  $\sim 10^3$ – $10^4$  s where stress approaches zero. At  $T \leq 50$  °C, there was no maximum relaxation time observed ( $\tau_{\text{relaxation}} > 10^5$  s).
4. Absorbed water slows down the stress relaxation of Nafion. At  $a_w = 1.0$ , there was no maximum relaxation time observed for  $23^\circ \leq T \leq 90^\circ \text{C}$ .
5. Imposed strain slows down the relaxation of Nafion. At 90 °C and  $a_w = 0$ , there was a finite relaxation time of  $10^3$  s for 5%

strain, but no upper limit to the relaxation time was observed for  $>10\%$  strain.

On the basis of the data we will argue that temperature, water absorption, and imposed strain can drive microphase separation in Nafion. When physical conditions drive ordered phase separation, the elastic modulus of Nafion increases and the relaxation processes become slower. When the ionic groups are in a disordered state, the elastic modulus decreases and relaxation occurs on a faster time scale.

### Effect of Water Absorption on the Elastic Modulus of Nafion

The results reported here for the elastic modulus as a function of temperature and water activity are in good agreement with those reported by Bauer et al.,<sup>4</sup> Uan-Zo-Li,<sup>18</sup> and Budinski et al.<sup>9</sup> All these studies indicated that Nafion was plasticized by water. They also saw the elastic modulus decreased more with temperature at low water activity than at high water activity and  $\sim 90$  °C the modulus of dry Nafion becomes less than the modulus of humidified Nafion. Bauer et al. also reported that low water activities increased the elastic modulus of Nafion, which we also found here. Many earlier studies had not seen the increase in elastic modulus with water activity; this was probably because of the difficulties in maintaining good environmental control.

The large decrease in elastic modulus with temperature around 80–90 °C for dry Nafion is well known.<sup>14,20,22,26,34,37,38,44,45</sup> Eisenberg provided an explanation for this transition as the balance between the electrostatic energy to form clusters of sulfonic acid groups opposed by the elastic energy to draw the sulfonic acid groups together.<sup>46</sup> The critical temperature,  $T_c$ , is where the entropic contributions of the elastic energy win out over the electrostatic bonding contributions. The transition between a microphase separated system and the random system as suggested by Eisenberg is illustrated schematically in Figure 13. Eisenberg's model included only nonspecific interactions between groups, producing a monotonic effect on the role of water; a more complicated model with specific hydrogen bonding interactions could produced the maximum in the elastic modulus with water activity.

Water is strongly attracted to the sulfonic acid groups but is repelled from the PTFE matrix. The

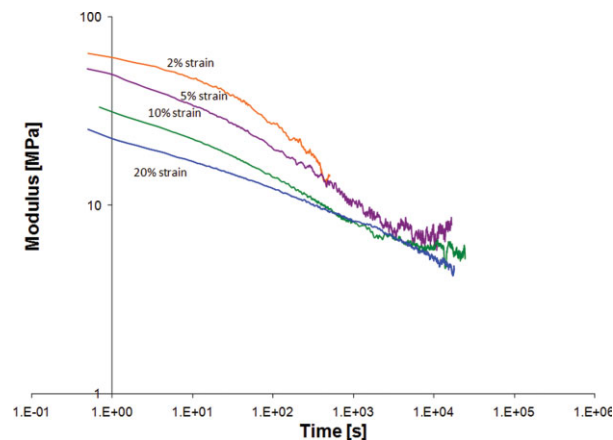


**Figure 12.** Stress relaxation of 1100 equivalent weight Nafion at 90 °C as a function of initial strain under wet conditions ( $\sim 100\%$  RH). [Color figure can be viewed in the online issue, which is available at [www.interscience.wiley.com](http://www.interscience.wiley.com).]

absorption of water will increase the bonding energy within the ionic cluster thus shifting the critical temperature where entropic contributions

win out higher. The absorption of water can drive the miscible system to phase separate.

Sulfonic acid groups from the same polymer molecule can be in two different clusters providing crosslinks, which stiffen Nafion. At dry conditions, the dipole interactions bind the sulfonic acid groups together. Adding a small amount of water into the clusters allows hydrogen bonding between the sulfonic acid groups, which increases the binding energy.<sup>4</sup> The yield stress corresponds to breaking crosslinks apart, overcoming the binding energy between sulfonic acid groups. The stronger hydrogen bonds increase the yield stress. As the water content increases further, the acid residues are solvated and they become like flexible joints in a socket (the cluster). The flexible joints give the effect of a stronger but more flexible interaction.

The results presented here also showed that water activity altered the yield stress in Nafion, even at low temperature. In her thesis, Satterfield also reported measurements of the toughness and “plastic” modulus of Nafion as functions of

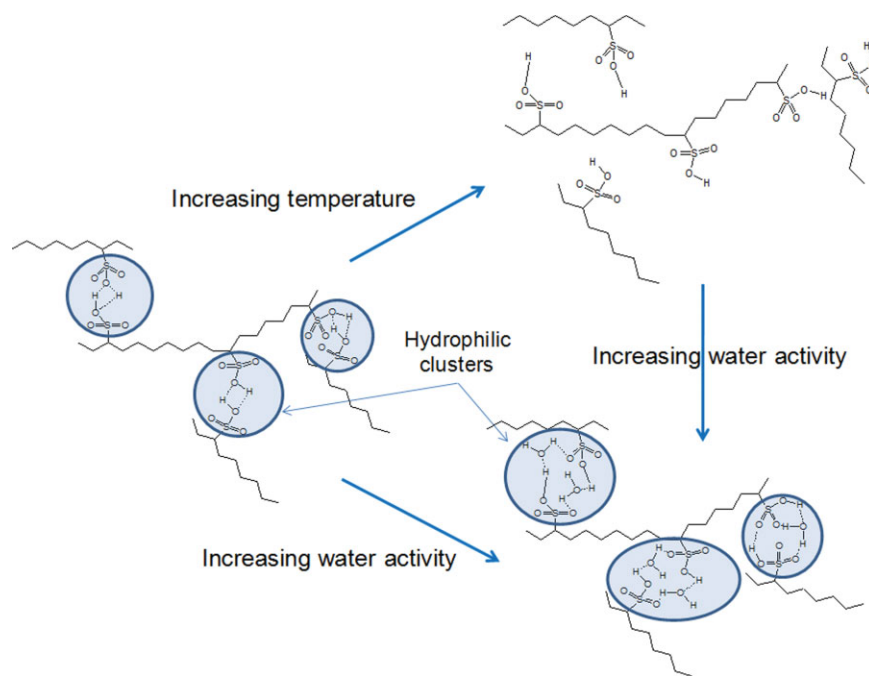


**Figure 13.** Schematic of the microphase evolution in Nafion as functions of temperature and water activity. The sulfonic acid groups cluster by a combination of polar interactions and hydrogen bonding. As the temperature is raised above a critical temperature (in the absence of absorbed water  $T_c \sim 90$  °C), the sulfonic acid clusters become miscible in the PTFE matrix reducing the elastic modulus. Water absorption solvates the sulfonic acid groups and creates hydrogen bonding within the clusters. The strong water/acid interactions stabilize the phase separation to a much higher critical temperature. [Color figure can be viewed in the online issue, which is available at [www.interscience.wiley.com](http://www.interscience.wiley.com).]

temperature and water activity. Those properties mirrored those seen with elastic modulus and yield point; we did not include those data here, but the interested reader can access those results on the web (<http://pemfc.princeton.edu/theses.html>).

### Stress Relaxation Process in Nafion

Stress relaxation is normally modeled as a superposition of viscoelastic elements with different relaxation times,  $\tau_i$ , as shown in eq 1. Most data is fit to a finite series of viscoelastic elements with relaxation times distributed between times  $\tau_{\min}$ , and  $\tau_{\max}$ .

$$E(t) = \sum_{i=1}^{\infty} E_i \exp\left[-\frac{t}{\tau_i}\right] \quad (1)$$

$\tau_{\min} < \tau_i < \tau_{\max}$

At times less than the maximum relaxation time, the stress decays slowly with time ( $t/\tau_{\max} < 1$ ),  $E \approx E_{\max}(\tau_{\max}-t)$ . For times greater than the maximum relaxation time, the stress approaches zero exponentially, ( $t/\tau_{\max} > 1$ ),  $E \rightarrow 0$ . This change in slope of  $\log(E)$  versus  $\log(t)$  is seen in Figure 7 at high temperatures ( $T \geq 70$  °C) with dry Nafion ( $a_w = 0$ ). This data is indicative of an upper limit to the relaxation time for Nafion. Dry Nafion ( $a_w = 0$ ) at 70 °C is above the critical temperature for microphase separation and the elastic modulus is low and there appears to be a finite upper limit to the stress relaxation time. When the temperature is reduced and phase separation produces a crosslinked structure with a high elastic modulus, there is no upper limit to the stress relaxation time.

We suggest that ordering in the microphase structure of Nafion slows down the stress relaxation rate. At high temperature and low water activity, the sulfonic acid groups are miscible in the PTFE matrix, there is no strong driving force for microstructural rearrangement, and the stress relaxes away in a finite time. However, when there is microphase separation, the driving force for order within the hydrophilic domains will drive for greater order so the relaxation process continues for much longer time.

The stress relaxation results at low water activity suggest two distinctly different modes of relaxation, relaxation in a miscible system with a finite upper limit to relaxation and relaxation in a microphase separated system where the relaxation shows no upper limit. When Nafion is

exposed to water vapor at low and high temperature no upper limit to the relaxation time is seen in Figures 7 and 8. This can be seen more clearly by constructing time–temperature and time–strain superposition curves. Figure 14 is the stress relaxation time–temperature superposition curve for Nafion at an initial strain of 5%. We have included the data at 0% RH, ambient air, and 100% RH. The shift factors as a function of temperature are shown in the upper right inset. At times  $< 10^3$  s, stress relaxation of Nafion is approximately independent of temperature and water activity, and all the stress relaxation curves show a similar correlation of modulus with time. At times  $> 10^4$  s, two distinctly different relaxation processes were observed. Several samples show a rapid drop in the modulus at a maximum relaxation time of  $\sim 2\text{--}5 \times 10^4$  s. These samples were at 0% RH or ambient RH and  $T \geq 70$  °C. In contrast, samples that were at 100% RH or at  $T \leq 50$  °C showed moduli that decayed slowly with increasing time. Figure 14 also suggests that the effect of temperature and water activity causes abrupt and distinct changes in the relaxation times. The time shifted data in Figure 14 indicates a jump in the characteristic relaxation rate between Nafion with absorbed water and Nafion at low temperature to Nafion at  $a_w = 0$  and high temperature. The time shifted data shows either a maximum relaxation time of  $10^4$  s or no upper limit to the relaxation time. This jump is suggestive of a change in phase.

The stress-relaxation time–temperature superposition suggests a transition in mechanical behavior that is a function of temperature and water activity. Figure 15 presents the stress relaxation time–strain superposition at 70 °C for different relative humidities (0% RH and 100% RH). Time–strain superposition also shows two distinctly different relaxation processes. Below  $10^3$  s, the relaxation appears to be independent of strain and water activity. At 2 and 5% initial strain with the dry and ambient RH, a limiting relaxation time is approached where the stress rapidly decreases. When the relative humidity was 100%, the modulus relaxed with no upper limit to the decay time. But at  $T \geq 70$  °C and  $a_w = 0$  when the initial strain was 10% or 20%, no upper limit to the relaxation time was observed. These results suggested that larger strain induced ordering in Nafion, which caused there to no longer be an upper limit to the relaxation time.

A number of investigators have seen isotropy in the ionomer peak SAXS peak for uniaxial

orientation at high water contents<sup>38,47–49</sup> and large draw ratios. Diat and coworkers did careful studies that showed increased intensity in the ionomer peak with uniaxial drawing.<sup>50–53</sup> Most of these studies were done at room temperature and did not account for the effects of temperature. Moore and coworkers used SAXS with alkyl ammonium cations to look at orientation with temperature and strain.<sup>38</sup> They showed that straining induced ordering of the ionomeric peak that could be erased by increasing the temperature. The temperature where ordering was erased appeared to be the same temperature where the storage modulus (determined by DMA) decreased. Elliott and coworkers showed that swelling by ethanol/water mixtures could also erase the anisotropy. In these studies, the imposed strain was  $>100\%$ , much greater than the strain tested in the experiments presented here.

Both time–temperature superposition and time–strain superposition results show two distinct responses—samples that show a limiting relaxation time (in the range of  $10^3$ – $10^4$  s) and samples that shown no limiting relaxation time (or the limiting relaxation time is  $>10^5$  s). The results show that relaxation time decreases with increasing temperature, decreasing water activity, and decreasing strain. However, the relaxation time did not change continuously with these parameters but changed abruptly. Because of the discontinuous change in relaxation, we suggest

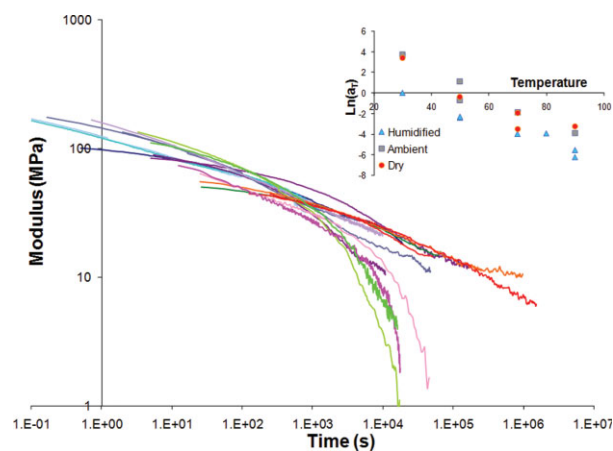


**Figure 14.** Time–temperature stress relaxation superposition for Nafion 115 initially strained to 5%. Stress relaxation curves from 23 to 90 °C at 0% RH, ambient RH, and 100% RH were time shifted to fall on a universal curve. The shift factors as a function of temperature are presented in the inset. [Color figure can be viewed in the online issue, which is available at [www.interscience.wiley.com](http://www.interscience.wiley.com).]

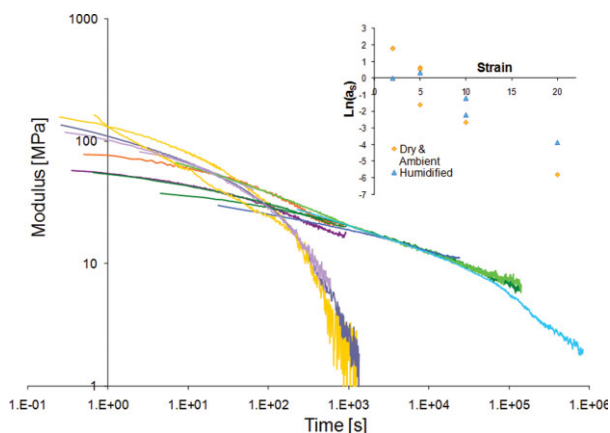


**Figure 15.** Stress relaxation time–strain superposition of Nafion at 70 °C at different water activities. [Color figure can be viewed in the online issue, which is available at [www.interscience.wiley.com](http://www.interscience.wiley.com).]

that these responses are the results of microphase restructuring induced by the combination of temperature, absorbed water, and applied stress acting in concert.

Stress relaxation results indicate that decreased temperature, increased water activity, and increased strain produced similar changes between two states of Nafion. Low temperature and low water activity is associated with a microphase separated system that showed no upper limit to its stress relaxation time. High temperature and low water activity has no phase separation and exhibits an upper limit to its stress-relaxation time. Increased water activity causes Nafion to microphase separate, resulting in no upper limit to its stress relaxation time. Our results have also suggested that strain may induce ordering in Nafion producing the same effects that temperature and water absorption produce in altering microphase separation.

## CONCLUSIONS

Tensile properties of 1100 equivalent weight Nafion have a complex dependence on temperature, water activity, and strain. The key results report here are:

1. At constant water activity, the elastic modulus of Nafion decreases with increasing temperature. The elastic modulus decreases faster with temperature at  $a_w = 0$  than at  $a_w = 1.0$ . Below 90 °C, the elastic modulus is greater at  $a_w = 0$ , and above

- 90 °C, the elastic modulus is greater at  $a_w = 1.0$ .
- Initial absorption of water  $0 < a_w < 0.3$  causes the elastic modulus and yield stress of Nafion to increase at both 23 and 90 °C. The elastic modulus of Nafion is a maximum at a water activity of  $\sim 0.3$ . Higher water activities cause both the elastic modulus and yield stress to decrease.
  - Stress relaxation in Nafion appears to be correlated with ordering of the hydrophilic sulfonic acid domains. At  $a_w = 0$ ,  $T \geq 70$  °C, and applied strain of  $< 5\%$ , Nafion has a low elastic modulus and relaxes with a maximum relaxation time of  $\sim 10^3$ – $10^4$  s. This maximum relaxation time appears to be correlated with lack of order for the sulfonic acid clusters.
  - Water absorption increases the upper limit to the relaxation time to exceed  $10^5$  s.
  - Stress relaxation of dry Nafion at 90 °C occurs with a maximum time constant of  $\sim 10^3$  s for small initial strains ( $< 5\%$ ). At initial strains of  $\geq 10\%$  the upper limit for the stress relaxation time exceeded  $10^5$  s.
  - Temperature  $< 90$  °C, water activity  $> 10\%$ , strain  $> 10\%$  all cause the stress relaxation time constant to show no upper limit and suggest those conditions induce microphase ordering.
  - Kundu, S.; Simon, L. C.; Fowler, M.; Grot, S. *Polymer* 2005, 46, 11707–11715.
  - Liu, D.; Hickner, M. A.; Case, S. W.; Lesko, J. J. *J Eng Mater Technol-Trans ASME* 2006, 128, 503–508.
  - Solasi, R.; Zou, Y.; Huang, X.; Reifsnider, K.; Condit, D. *J Power Sources* 2007, 167, 366–377.
  - Budinski, M.; Gittleman, C. S.; Lai, Y. H.; Litteer, B.; Miller, D. In *AIChE Annual Meeting: Austin, TX, 2004*. Presentation slides used at 2004 AIChE Annual Meeting.
  - Choi, P.; Jalani, N. H.; Thampan, T. M.; Datta, R. *J Polym Sci Part B-Polym Phys* 2006, 44, 2183–2200.
  - Liu, Y. H.; Yi, B. L.; Shao, Z. G.; Xing, D. M.; Zhang, H. M. *Electrochem Solid State Lett* 2006, 9, A356–A359.
  - Greso, A. J.; Moore, R. B.; Cable, K. M.; Jarrett, W. L.; Mauritz, K. A. *Polymer* 1997, 38, 1345–1356.
  - Satterfield, M. B.; Majsztrik, P. W.; Ota, H.; Benziger, J. B.; Bocarsly, A. B. *J Polym Sci B: Polym Phys* 2006, 44, 2327–2345.
  - Choi, P.; Jalani, N. H.; Datta, R. *J Electrochem Soc* 2005, 152, E84–E89.
  - Newns, A. C. *Trans Farad Soc* 1956, 52, 1533–1545.
  - Rivin, D.; Kendrick, C. E.; Gibson, P. W.; Schneider, N. S. *Polymer* 2001, 42, 623–635.
  - Morris, D. R.; Sun, X. *J Appl Polym Sci* 1993, 50, 1445–1452.
  - Uan-Zo-li, J. T. In *Materials Science and Engineering*; Virginia Polytechnic Institute and State University: Blacksburg, Virginia, 2001, p 117.
  - Werner, S.; Jorissen, L.; Heider, U. *Ionics* 1996, 2, 19–23.
  - Kyu, T.; Eisenberg, A. *ACS Sympos Ser* 1982, 180, 79–110.
  - Kyu, T.; Eisenberg, A. *J Polym Sci-Polym Symposia* 1984, 203–219.
  - Yeo, S. C.; Eisenberg, A. *J Appl Polym Sci* 1977, 21, 875–898.
  - Krtil, P.; Trojanek, A.; Samec, Z. *J Phys Chem B* 2001, 105, 7979–7983.
  - Takamatsu, T.; Hashiyama, M.; Eisenberg, A. *J Appl Polym Sci* 1979, 24, 2199–2220.
  - Bagley, E.; Long, F. A. *J Am Chem Soc* 1955, 77, 2172–2178.
  - Jalani, N. H.; Mizar, S. P.; Choi, P.; Furlong, C.; Datta, R. *Proc SPIE* 2004, 5532, 316–325.
  - Jalani, N. H.; Choi, P.; Datta, R. *J Membr Sci* 2005, 254, 31–38.
  - DuPont. Wilmington, DE, 2006, p 4.
  - Kawano, Y.; Wang, Y. Q.; Palmer, R. A.; Aubuchon, S. R. *Polimeros: Ciencia e Tecnologia* 2002, 12, 96–101.
  - Fujimoto, C. H.; Hickner, M. A.; Cornelius, C. J.; Loy, D. A. *Macromolecules* 2005, 38, 5010–5016.

The authors thank the National Science Foundation (CTS-0354279 and DMR-0213707 through the Materials Research and Science Engineering Center at Princeton) for support of this work.

## REFERENCES AND NOTES

- Hector, L. G.; Lai, Y. H.; Tong, W.; Lukitsch, M. J. *J Fuel Cell Sci Technol* 2007, 4, 19–28.
- Huang, X. Y.; Solasi, R.; Zou, Y.; Feshler, M.; Reifsnider, K.; Condit, D.; Burlatsky, S.; Madden, T. *J Polym Sci Part B-Polym Phys* 2006, 44, 2346–2357.
- Tang, Y. L.; Karlsson, A. M.; Santare, M. H.; Gilbert, M.; Cleghorn, S.; Johnson, W. B. *Mat Sci Eng A: Struct Mater Propert Microstruct Process* 2006, 425, 297–304.
- Bauer, F.; Denneler, S.; Willert-Porada, M. *J Polym Sci Part B-Polym Phys* 2005, 43, 786–795.
- Liu, D.; Kyriakides, S.; Case, S. W.; Lesko, J. J.; Li, Y. X.; McGrath, J. E. *J Polym Sci Part B-Polym Phys* 2006, 44, 1453–1465.

31. Kyriakides, S. A. *J Undergrad Mater Res* 2005, 1, 11–14.
32. Takamatsu, T.; Eisenberg, A. *J Appl Polym Sci* 1979, 24, 2221–2235.
33. Jalani, N. H.; Dunn, K.; Datta, R. *Electrochimica Acta* 2005, 51, 553–560.
34. Kim, Y. M.; Choi, S. H.; Lee, H. C.; Hong, M. Z.; Kim, K.; Lee, H. I. *Electrochimica Acta* 2004, 49, 4787–4796.
35. Park, Y. S.; Yamazaki, Y. *J Membr Sci* 2005, 261, 58–66.
36. Shao, Z. G.; Xu, H. F.; Li, M. Q.; Hsing, I. M. *Solid State Ionics* 2006, 177, 779–785.
37. Hodge, I. M.; Eisenberg, A. *Macromolecules* 1978, 11, 289–293.
38. Page, K. A.; Landis, F. A.; Phillips, A. K.; Moore, R. B. *Macromolecules* 2006, 39, 3939–3946.
39. Majsztzik, P. W.; Bocarsly, A. B.; Benziger, J. B. *Rev Scientific Instr* 2007, 78.
40. Majsztzik, P. W. In *Chemistry*; Princeton University: Princeton, NJ, 2008, p 235.
41. Yang, C.; Srinivasan, S.; Bocarsly, A. B.; Tulyani, S.; Benziger, J. B. *J Membr Sci* 2004, 237, 145–161.
42. In *CRC Handbook of Chemistry and Physics*, Internet Version 2007; Lide, D. R.; Ed.; Taylor and Francis: Boca Raton, FL, 2007, pp 6–92.
43. Wexler, A. In *CRC Handbook of Chemistry and Physics*, Internet Version 2007; Lide, D. R.; Ed.; Taylor and Francis: Boca Raton, FL, 2007, pp 15–33.
44. Mauritz, K. A.; Moore, R. B. *Chem Rev* 2004, 104, 4535–4585.
45. Osborn, S. J.; Hassan, M. K.; Divoux, G. M.; Rhoades, D. W.; Mauritz, K. A.; Moore, R. B. *Macromolecules* 2007, 40, 3886–3890.
46. Eisenberg, A.; Kim, J.-S. In *Introduction to Ionomers*; John Wiley & Sons, Inc.: New York, 1998, pp 164–189.
47. Elliott, J. A.; Hanna, S.; Elliott, A. M. S.; Cooley, G. E. *Macromolecules* 2000, 33, 4161–4171.
48. Elliott, J. A.; Hanna, S.; Elliott, A. M. S.; Cooley, G. E. *Polymer* 2001, 42, 2251–2253.
49. Londono, J. D.; Davidson, R. V.; Mazur, S. *Abstr Pap Am Chem Soc* 2001, 222, U342.
50. Rollet, A. L.; Diat, O.; Gebel, G. *J Phys Chem B* 2002, 106, 3033–3036.
51. Rubatat, L.; Diat, O. *Macromolecules* 2007, 40, 9455–9462.
52. Rubatat, L.; Gebel, G.; Diat, O. *Macromolecules* 2004, 37, 7772–7783.
53. van der Heijden, P. C.; Rubatat, L.; Diat, O. *Macromolecules* 2004, 37, 5327–5336.